

1 **GWAS of 19,629 individuals identifies novel genetic variants for regional**
2 **brain volumes and refines their genetic co-architecture with cognitive and**
3 **mental health traits**

4

5 **Running title: GWAS of 101 ROI volumes**

6

7 Bingxin Zhao, M.S.¹, Tianyou Luo, B.S.¹, Tengfei Li, Ph.D.^{2,3}, Yun Li, Ph.D.^{1,4,5}, Jingwen
8 Zhang, Ph.D.⁶, Yue Shan, M.S.¹, Xifeng Wang, B.S.¹, Liuqing Yang, M.S.⁷, Fan Zhou, M.S.¹,
9 Ziliang Zhu, B.S.¹, and Hongtu Zhu, Ph.D.*¹

10

11 ¹ Departments of Biostatistics, ² Radiology, ⁴ Computer Science, ⁵ Genetics, and ⁷
12 Statistics and Operations Research, University of North Carolina at Chapel Hill, Chapel
13 Hill, NC, USA, 27599

14 ³ Biomedical Research Imaging Center, School of Medicine, The University of North
15 Carolina at Chapel Hill, Chapel Hill, NC, USA, 27599

16 ⁶ Department of Biostatistics, T.H. Chan School of Public Health, Harvard University,
17 Boston, MA, USA, 02115

18

19 **Corresponding author:*

20 Hongtu Zhu

21 Department of Biostatistics, University of North Carolina at Chapel Hill,
22 3105C McGavran-Greenberg Hall, Chapel Hill, NC 27599.

23 Email address: htzhu@email.unc.edu Phone: (919) 966-7250

24

25 List of Alzheimer's Disease Neuroimaging Initiative (ADNI) and Pediatric Imaging,
26 Neurocognition and Genetics (PING) authors provided in the supplemental materials.

27

28

29

30

31

32 Version: March 21, 2019

1 **Abstract**

2 Volumetric variations of human brain are heritable and are associated with many
3 brain-related complex traits. Here we performed genome-wide association studies
4 (GWAS) and post-GWAS analyses of 101 brain volumetric phenotypes using the UK
5 Biobank (UKB) sample including 19,629 participants. GWAS identified 287 independent
6 SNPs exceeding genome-wide significance threshold of 4.9×10^{-10} , adjusted for testing
7 multiple phenotypes. Gene-based association study found 142 associated genes (113
8 new) and functional gene mapping analysis linked 122 more genes. Many of the
9 discovered genetic variants have previously been implicated with cognitive and mental
10 health traits (such as cognitive performance, education, mental disease/disorders), and
11 significant genetic correlations were detected for 29 pairs of traits. The significant SNPs
12 discovered in the UKB sample were supported by a joint analysis with other four
13 independent studies (total sample size 2,192), and we performed a meta-analysis of five
14 samples to provide GWAS summary statistics with sample size larger than 20,000. Using
15 genome-wide polygenic risk scores prediction, up to 4.36% of phenotypic variance
16 ($p\text{-value}=2.97 \times 10^{-22}$) in the four independent studies can be explained by the UKB GWAS
17 results. In conclusion, our study identifies many new genetic variants at SNP, locus and
18 gene levels and advances our understanding of the pleiotropy and genetic
19 co-architecture between brain volumes and other traits.

20

21 **Keywords:** Genetic co-architecture; Genetic correlation; Pleiotropy; UK Biobank; Brain
22 structure; Regional brain volumes.

23

24

25

26

27

28

29

30

31

1 Regional brain volumes are heritable measures of brain functional and structural
2 changes. Volumetric variations of human brain are known to be phenotypically and
3 genetically associated with heritable cognitive and mental health traits (1-5), and it is an
4 active research area to understand the shared genetic influences in these traits (6).
5 Individual variations of human brain volume are usually quantified by magnetic
6 resonance imaging (MRI). In region of interest (ROI)-based analysis, whole brain MRIs
7 are processed and annotated onto many pre-defined ROIs, and then regional volumetric
8 phenotypes are generated to measure the structure of brain ROIs. Family and
9 population-based studies have both shown that these volumetric phenotypes are highly
10 heritable (7-9), and common single-nucleotide polymorphism (SNP) markers collected
11 across the genome can account for a large proportion of phenotypic variation (10). A
12 highly polygenic or omnigenic (11, 12) genetic architecture has been observed, which
13 indicates that a large number of genetic variants influence regional brain volumes and
14 their genetic contributions are widespread across the whole genome.

15

16 Several genome-wide association studies (GWAS) (3, 7, 8, 13-18) have been conducted
17 to identify genetic risk variants for brain volumetric phenotypes. However, except for
18 the whole brain volume and volumes of few specific ROIs (e.g., hippocampus in
19 subcortical area (3, 8, 19)), GWAS of most brain volumetric phenotypes were
20 insufficiently powered, for which the largest sample size of discovery GWAS was less
21 than 10,000 in (7). Such GWAS sample size is much smaller than those of recent GWAS
22 of other heritable brain-related traits, such as cognitive function (20), neuroticism (21),
23 and intelligence (22), where sample sizes ranged from 269,867 to 449,484. Given the
24 polygenic nature of brain volumes, most of the genetic risk variants may remain
25 undetected, and GWAS with larger sample size can uncover more associated variants
26 and enrich the pleiotropy and genetic co-architecture with other traits. Recently, the UK
27 Biobank (UKB, (23)) study team has collected and released MRI data for more than
28 20,000 participants. In addition, publicly available imaging genetic datasets also emerge
29 from several other independent studies, including Philadelphia Neurodevelopmental
30 Cohort (PNC, (24)), Alzheimer's Disease Neuroimaging Initiative (ADNI, (25)), Pediatric
31 Imaging, Neurocognition, and Genetics (PING, (26)), and the Human Connectome

1 Project (HCP,(27)), among others. These datasets provide a new opportunity to perform
2 better-powered GWAS of all ROI brain volumes.

3

4 Here we downloaded the raw MRI data from these data resources and processed the
5 data using consistent standard procedures via advanced normalization tools (ANTs, (28))
6 to generate 101 regional (and total) brain volume phenotypes (referred as ROI volumes),
7 including the total brain volume (TBV), gray matter (GM), white matter (WM), and
8 cerebrospinal fluid (CSF). 19,629 UKB individuals of British ancestry were used in the
9 main discovery GWAS. Other four datasets with relatively small sample sizes (total
10 sample size 2,192 after quality controls) were used to validate the UKB findings and
11 finally a meta-analysis was performed to combine all the data. We started our analysis
12 of UKB data with estimating the SNP heritability, which is the proportion of phenotypic
13 variation that can be explained by the additive effects of all common autosomal SNPs
14 (29). Particularly, the UKB MRI data were released at different time points. We
15 organized them in two parts: the first part was released in 2017 (referred as phase 1 in
16 this paper, n=9,198), most of which has been analyzed in (7), and the second part was
17 released in 2018 (referred as phase 2, n=10,431). To detect any potential heterogeneity
18 of the two phases, we compared the SNP heritability estimated in phase 2 data to those
19 in phase 1 data, which were reported in (10). We then carried out GWAS to identify the
20 associated genetic variants for each ROI volume. We performed gene-based association
21 analysis via MAGMA (30) to uncover gene-level associations, and performed post-GWAS
22 functional mapping and annotation (FUMA, (31)) to explore the functional
23 consequences of the significant SNPs. We calculated the pairwise genetic correlation
24 between ROI volumes and 50 brain-related complex traits by the LD score regression
25 (LDSC, (32)). To confirm the robustness of UKB GWAS findings, we jointly analyzed the
26 UKB GWAS results with those from PNC, ADNI, PING and HCP. We developed
27 genome-wide polygenic risk scores (PRS) to assess the predictive ability of the UKB
28 GWAS results on the other four datasets. GWAS summary statistics of the UKB sample
29 and meta-analysis for the five studies have been made available to public at
30 <https://med.sites.unc.edu/big2/data/gwas-summary-statistics/>.

31

32 **RESULTS**

1 **SNP heritability estimates of the two UKB phases data**

2 **Supplementary Fig. 1** compares the SNP heritability (h^2) estimated separately from UKB
3 phase 1 and 2 data. The correlation of these estimates was 0.79, indicating moderate to
4 high level of agreement in terms of the degree of genetic contributions to ROI between
5 the two phases. Six ROIs had >0.6 h^2 estimates in both phases, including TBV, cerebellar
6 vermal lobules VIII-X, cerebellar vermal lobules I-V, brain stem, and left/right cerebellum
7 exterior. The h^2 estimates from the combined data were highly correlated with those
8 from phase 1 (correlation=0.91) and phase 2 (correlation=0.92) (**Supplementary Figs.**
9 **2-3**). The SNP heritability estimates, standard errors, raw and Bonferroni-corrected
10 p-values from the one-sided likelihood ratio tests are provided in **Supplementary Table**
11 **1**. Significant genetic controls widely spread across most ROIs of the whole brain (mean
12 $h^2=0.35$, h^2 range=[0.15,0.71], standard error=0.15). Heritability of left/right basal
13 forebrain ($h^2=0.09/0.11$) and optic chiasm ($h^2=0.01$) were insignificant.

14

15 **Significant GWAS associations of 101 ROI volumes**

16 We carried out GWAS of the 101 ROI volumes with using 8,944,375 SNPs after
17 genotyping quality controls. Manhattan and QQ plots of all the 101 phenotypes are
18 displayed in **Supplementary Fig. 4**. There were 22,353 significant associations at the
19 conventional $5*10^{-8}$ GWAS significance level and 12,060 significant ones at the $4.9*10^{-10}$
20 significance level (that is, $5*10^{-8}/101$, additionally adjusted for all 101 GWAS performed)
21 (**Supplementary Fig. 5, Supplementary Table 2**). TBV had the largest number of
22 significant associations, which was 3,408 at $4.9*10^{-10}$ significance level. In addition to
23 TBV, left/right hippocampus, left/right putamen, and cerebellar vermal lobules VIII-X
24 had more than 500 significant associations. In the rest of this paper, we refer $4.9*10^{-10}$
25 as the significance threshold for SNP-level associations unless otherwise stated.

26

27 287 independent significant SNPs had 392 significant associations with 54 ROIs
28 (**Supplementary Table 3**). Independent significant SNPs were defined as significant SNPs
29 that were independent of other significant SNPs by FUMA (Online Methods, (31)). The
30 number of associations for each ROI is displayed in **Figure 1 and Supplementary Table 4**.
31 Left/right hippocampus, cerebellar vermal lobules VIII-X, left/right putamen, and
32 cerebellar vermal lobules I-V had at least 19 independent significant SNPs. Other ROIs

1 that had at least 10 independent significant SNPs included left/right precentral, brain
2 stem, X4th ventricle, left/right lateral ventricle, left/right cerebellum white matter, and
3 TBV. The number of independent significant associations on each chromosome is shown
4 in **Supplementary Table 5**, and clearly chromosome 12 had the largest number of
5 SNP-level associations with ROI volumes (**Supplementary Fig. 6**).

6
7 The 392 independent significant SNP-level associations can be further characterized
8 (Online Methods) as 134 significant associations between genetic risk loci and ROI
9 volumes (**Table 1, Supplementary Table 6**). Brain stem, cerebellar vermal lobules VIII-X,
10 left/right lateral ventricle, TBV and WM had at least five genetic risk loci
11 (**Supplementary Table 7**). Each chromosome had at least one genetic risk locus except
12 for chromosomes 13 and 21 (**Supplementary Tables 8**). Results at significance
13 thresholds 5×10^{-8} and 5×10^{-9} are also provided in above tables and are summarized in
14 **Supplementary Table 9**.

15

16 **Concordance with previous GWAS results**

17 We performed association lookups for the 287 independent significant SNPs and their
18 correlated SNPs in genetic risk loci (Online Methods) on the NHGRI-EBI GWAS catalog
19 (33). We found that 117 independent significant SNPs (associated with 36 ROI volumes)
20 have previously reported GWAS associations with any traits (**Supplementary Table 10**).
21 Our results tagged many SNPs that were previously reported in GWAS of ROI volumes,
22 including 14 SNPs in van der Meer, Rokicki (3) for hippocampal subfield volumes, 11 in
23 Hibar, Stein (8) for subcortical brain region volumes, 5 in Chen, Wang (34) for putamen
24 volume, 4 in Bis, DeCarli (18) for hippocampal volume, 2 in Hibar, Adams (14) for
25 hippocampal volume, 2 in Stein, Medland (35) for brain structure, 2 in Ikram, Fornage
26 (17) for intracranial volume, 1 in Furney, Simmons (36) for whole brain volume, and 1 in
27 Baranzini, Wang (37) for normalized brain volume (**Supplementary Table 11**). For the
28 other traits, we highlighted previous associations of 29 different SNPs with mental
29 health disease/disorders (such as schizophrenia, autism spectrum disorder [ASD], and
30 depression), 78 with cognitive functions, 17 with educational attainment, 20 with
31 neuroticism, 14 with Parkinson's disease, 3 with reaction time, and 1 with Alzheimer's
32 disease. More previous GWAS results were found when the significance threshold was

1 relaxed to 5×10^{-8} (**Supplementary Table 12**). We also compared our results with those
2 reported in (7). Elliott, Sharp (7) performed GWAS of 3,144 imaging phenotypes
3 (including brain volume phenotypes processed by FreeSurfer (38)) using the UKB phase
4 1 data ($n=8,428$). When both being corrected for the number of performed GWAS, 26 of
5 the 78 unique SNPs (covered 66 of the 368 significant associations) reported in (7) were
6 within LD of our independent significant SNPs (**Supplementary Table 13**). When both
7 being relaxed to the 5×10^{-8} significance threshold, 119 of their 616 unique SNPs
8 (covered 493 of the 1,262 significant associations) were within LD of our independent
9 significant SNPs.

10

11 **Gene-based association analysis and functional mapping**

12 We performed gene-based association analysis with GWAS summary statistics for
13 18,796 candidate genes (Online Methods). We found 237 significant gene-level
14 associations ($p\text{-value} < 2 \times 10^{-8}$, adjusted for multiple traits) between 142 genes and 47
15 ROIs (**Table 2, Supplementary Table 14**). Our results replicated 29 genes discovered in
16 previous studies, including *FOXO3* in Baranzini, Wang (37), *HMG2* and *HRK* in Stein,
17 Medland (35), *KANSL1*, *MAPT*, *STH* and *CENPW* in Ikram, Fornage (17), *SLC44A5* in
18 Furney, Simmons (36), *MSRB3*, *BCL2L1*, *DCC*, *CRHR1* in Hibar, Stein (8), *LEMD3*, *WIF1* and
19 *ASTN2* in Bis, DeCarli (18), *FAM53B*, *METTL10* and *FAF1* in van der Meer, Rokicki (3),
20 *DSCAML1* in Chen, Wang (34), *SLC39A1*, *GATAD2B*, *DENND4B* in Hibar, Stein (39), and
21 *ZIC4*, *VCAN*, *PAPPA*, *DRAM1*, *GNPTAB*, *DAAM1*, and *ALDH1A2* in Elliott, Sharp (7). 13
22 genes were novel and were not linked to ROI volumes. 57 genes have previously been
23 implicated with cognitive functions, intelligence, education, neuroticism,
24 neuropsychiatric and neurodegenerative diseases/disorders, such as *IGF2BP1* (22, 40,
25 41), *WNT3* (20, 21, 42, 43), *PLEKHM1* (43-45), and *AGBL2* (21, 43, 46, 47). Particularly, 40
26 of the 57 pleiotropic genes were novel genes of ROI volumes, and thus these findings
27 substantially uncovered the gene-level pleiotropy between ROI volumes and these traits
28 (**Figure 2**).

29

30 The independent significant SNPs were also annotated by functional consequences on
31 gene functions (**Supplementary Table 15, Supplementary Fig. 7**), and were
32 subsequently mapped to genes according to physical position, expression quantitative

1 trait loci (eQTL) association (for brain tissues), and 3D chromatin (Hi-C) interaction
2 (Online Methods). Functional gene mapping yielded 389 significant associations on 214
3 genes and 49 ROIs (**Supplementary Table 16**). 122 genes were not discovered in the
4 above gene-based association analysis, which replicated more previous findings on ROI
5 volumes, such as *TBPL2* and *KTN1* in Chen, Wang (34), *FAT3* in Hibar, Stein (8), *SLC4A10*,
6 *RNFT2*, *TESC*, *DMRTA2*, *CDKN2C* and *DPP4* in van der Meer, Rokicki (3), and *EPHA3*,
7 *SLC39A8*, *BANK1*, *WNT16*, *CHPT1*, *ACADM*, *FAM3C*, *FBXW8*, *L3HYPDH*, *JKAMP*, and *AQP9*
8 in Elliott, Sharp (7). 31 (23 new) of the 122 genes were associated with cognitive
9 functions, intelligence, education, neuroticism, neuropsychiatric and neurodegenerative
10 disorders, such as *NT5C2* (21, 44, 48, 49), *ADAM10* (49, 50), and *GOSR1* (20, 44)
11 (**Supplementary Fig. 8**).

12

13 Gene-priority analysis was performed for 14 brain tissues to examine whether the
14 tissue-specific gene expression levels were related to the associations between genes
15 and ROI volumes (Online Methods). After adjusting for multiple testing (that is,
16 $14 \times 101 = 1,414$ tests) by the Benjamini-Hochberg (B-H) procedure (51) at 0.05 level, we
17 detected nine significant associations, including gene expression in brain hippocampus
18 tissue and gene's association significance with left hippocampus volume, and gene
19 expression in brain cerebellar hemisphere and cerebellum tissues and gene's association
20 significance with pallidum and putamen volumes ($p\text{-value} < 2.46 \times 10^{-4}$) (**Supplementary**
21 **Table 17**). These results showed that genes with higher transcription levels on these
22 brain tissues also had stronger associations with the corresponding brain ROI volumes.

23

24 **Joint analysis with four independent datasets**

25 To validate the UKB GWAS results, we repeated GWAS of 101 ROI volumes separately on
26 data obtained from four other independent studies: PNC (n=537), HCP (n=334), PING
27 (n=461), and ADNI (n=860). Due to the small sample size of these four datasets, the
28 probability of replicating significant findings in the UKB was low. Instead, we checked
29 whether the SNP effect signs were concordant in the five studies and whether the
30 p-value of top UKB SNPs decreased after meta-analysis (Online Methods). Smaller
31 p-values after meta-analysis indicates similar SNP effects in independent samples (52,
32 53).

1

2 The joint analysis was carried out on 3,841,911 SNPs which were present in all five sets
3 of GWAS results. For the 5,940 significant associations (at 4.9×10^{-10} significance level),
4 64.6% (3,839) associations had the same effect signs across the five studies, and 97.5%
5 (5,791) associations had the same effect signs in at least four studies (including UKB).
6 94.0% (1,880) of the top 2,000 significant associations had smaller p-value after
7 meta-analysis, and 92.3% (5,484) of all the 5,940 associations were enhanced. We then
8 performed meta-analysis on all the 8,944,375 UKB GWAS SNPs (SNPs were allowed to
9 be missing in the four independent datasets). There were more significant associations
10 after meta-analysis: 25,083 significant associations at 5×10^{-8} significance level and
11 14,004 at 4.9×10^{-10} significance level (**Supplementary Table 18, Supplementary Fig. 9**).

12

13 **Genetic correction with other traits**

14 The meta-analysis GWAS results were used to estimate the genetic correlation (*gc*) with
15 other traits via LDSC (32). As positive controls, we first estimated the genetic correlation
16 between several UKB ROIs volumes (TBV, left/right thalamus proper, left/right caudate,
17 left/right putamen, left/right pallidum, left/right hippocampus, left/right accumbens
18 area) and their corresponding traits studied in the ENIGMA consortium (54). The *gc*
19 estimates were all significant ($p\text{-value} < 1.20 \times 10^{-5}$) and average correlation was 0.93
20 (**Supplementary Table 19**). We then collected 50 sets of publicly available GWAS
21 summary statistics (**Supplementary Table 20**) and calculated their pairwise genetic
22 correlation with ROI volumes (**Supplementary Tables 21**). We mainly focused on traits
23 that showed evidence of pleiotropy in association lookups. There were 29 significant
24 associations after adjusting for multiple testing (4,900 tests) by the B-H procedure at
25 0.05 level (**Supplementary Tables 22, Supplementary Fig. 10**).

26

27 Significant genetic correlations linked 16 ROI volumes with general cognitive functions,
28 education (education years, college completion), intelligence, numerical reasoning,
29 reaction time, depressive symptoms, neuroticism, worry, ASD, and bipolar disorder (BD)
30 (**Figure 3**), which matched our findings in SNP and gene level lookups. Particularly, TBV
31 had positive correlations with cognitive functions, education, intelligence, and numerical
32 reasoning (*gc* range=[0.20,0.24], mean=0.22, *p*-value range=[1.54×10^{-11} , 2.73×10^{-5}]). Left

1 posterior cingulate showed positive correlations with cognitive functions, intelligence,
2 and numerical reasoning (gc range=[0.16,0.17], p-value range=[6.09×10^{-5} , 1.85×10^{-4}]).
3 We note that TBV has been adjusted in GWAS of ROIs other than TBV. Right rostral
4 anterior cingulate showed positive correlation with ASD (gc=0.32, p-value= 2.00×10^{-4}),
5 left rostral middle frontal had positive correlation with BD (gc=0.20, p-value= 1.00×10^{-4}),
6 and right precuneus had positive correlation with neuroticism (gc=0.17,
7 p-value= 1.20×10^{-4}). Reaction time had positive genetic correlations with left/right lateral
8 ventricle and X3rd ventricle (gc range=[0.16,0.18], p-value range=[3.13×10^{-5} , 1.58×10^{-4}]),
9 and had negative correlations with left/right pallidum, left/right ventral DC, and white
10 matter (gc range=[-0.20, -0.15], p-value range=[3.64×10^{-7} , 1.44×10^{-5}]). Negative genetic
11 correlations were also found on depressive symptoms (gc=-0.25, p-value= 3.33×10^{-5}),
12 neuroticism (gc=-0.14, p-value= 2.20×10^{-4}), and worry (gc=-0.14, p-value= 2.94×10^{-4}).

13

14 **Predictive ability of the UKB GWAS results**

15 We examined the out-of-sample prediction power of the UKB GWAS summary statistics
16 using polygenic risk scores prediction (55). We focused the analysis on total brain
17 volume. We first used a ten-fold cross-validation design to examine the prediction
18 power within the UKB sample (Online Methods). Five polygenic profiles were created
19 with p-value thresholds 1, 0.5, 0.05, 5×10^{-4} and 5×10^{-8} , respectively, and we examined
20 the incremental R-squared (Online Methods). The PRS can explain 1.51% of the variance
21 in total brain volume (p-value= 4.42×10^{-110}) (**Supplementary Table 23**). We then used the
22 GWAS summary statistics of 19,629 UKB individuals to construct polygenic profiles on
23 subjects in PNC, HCP, PING, and ADNI. The UKB-derived PRS were all significantly
24 associated with the phenotype in all the four independent datasets, and can account for
25 1.38%-4.36% phenotypic variation (p-value range=[2.97×10^{-22} , 1.44×10^{-6}]). The largest
26 R-squared 4.36% was in PNC dataset with threshold 1 and 224,657 SNP predictors.

27

28 **DISCUSSION**

29

30 In this study, we presented GWAS of 101 ROI volumes using data of 19,629 UKB
31 individuals. Our novel contributions include 1) identification of many newly associated
32 genetic variants at SNP, locus, and gene levels; 2) revealing the genetic co-architecture

1 of brain volume phenotypes and other brain-related complex traits; 3) validation of the
2 UKB results in independent studies; and 4) assessment of the predictive power of UKB
3 GWAS results. Significant ($p\text{-value} < 4.9 \times 10^{-10}$) associations were found for 54 of the 101
4 ROIs. With larger sample size, the present study replicated many known genetic variants
5 but also prioritized new ones. Compared to (7), our GWAS not only discovered more
6 genetic variants, but also enriched the degree of (statistical) pleiotropy (56) of the
7 associated genes and characterized the shared genetic influences with cognitive and
8 mental health traits.

9

10 However, the current GWAS sample size of ROI volumes (and many other brain imaging
11 phenotypes) is still far from being sufficient. The highly polygenic genetic architecture of
12 ROI volumes requires a larger number of subjects to identify many weak causal SNPs. In
13 the era of sharing GWAS summary statistics, well powered GWAS is essential for ROI
14 volumes to be linked to the genetic co-architecture atlas with other complex traits. For
15 example, a recent study of Watanabe, Stringer (56) to discover the global overview of
16 genetic co-architecture of 2,965 traits only focused on GWAS with sample size larger
17 than 50,000, with the average sample size of selected traits being 256,276. In our
18 genetic correlation analysis, we only obtained limited number of significant correlations,
19 even though many pleiotropic genes were found in association lookups. Therefore, we
20 expect that GWAS of ROI volumes with larger sample size will be available and can
21 further improve our understating of genetic overlaps underlying other traits. Besides
22 increasing the sample size, combining SNP data with external omic information, such as
23 gene expression data (57), may also help elucidate the causal mechanism, improve the
24 prediction performance of SNP data and reveal the genetic connections among traits.

25

26 **URLs.**

27 ANTs, <http://stnava.github.io/ANTs/>;
28 PLINK, <https://www.cog-genomics.org/plink2/> ;
29 GCTA, <http://cnsgenomics.com/software/gcta/> ;
30 METAL, <https://genome.sph.umich.edu/wiki/METAL>;
31 FUMA, <http://fuma.ctglab.nl/>;
32 MGAMA, <https://ctg.cncr.nl/software/magma>;

- 1 LD Score Regression, <https://github.com/bulik/ldsc/> ;
- 2 LD Hub, <http://ldsc.broadinstitute.org/ldhub/>;
- 3 MaCH-Admix, <http://www.unc.edu/~yunmli/MaCH-Admix> ;
- 4 NHGRI-EBI GWAS Catalog, <https://www.ebi.ac.uk/gwas/home>;
- 5 The atlas of GWAS Summary Statistics, <http://atlas.ctglab.nl/>;
- 6 UK Biobank, <http://www.ukbiobank.ac.uk/resources/> ;
- 7 PING, <http://pingstudy.ucsd.edu/resources/genomics-core.html> ;
- 8 PNC,
- 9 https://www.ncbi.nlm.nih.gov/projects/gap/cgi-bin/study.cgi?study_id=phs000607.v1.p
- 10 [1](#);
- 11 ADNI, <http://adni.loni.usc.edu/data-samples/>;
- 12 HCP, <https://www.humanconnectome.org/>.

13

14 **METHODS**

15 Methods are available in the **Online Methods** section.

16 *Note: One supplementary information pdf file and one supplementary zip file are*

17 *available.*

18

19 **ACKNOWLEDGEMENTS**

20 This research was partially supported by U.S. NIH grants MH086633 and MH116527, and

21 a grant from the Cancer Prevention Research Institute of Texas. We thank the

22 individuals represented in the UK Biobank, ADNI, HCP, PING and PNC datasets for their

23 participation and the research teams for their work in collecting, processing and

24 disseminating these datasets for analysis. This research has been conducted using the

25 UK Biobank resource (application number 22783), subject to a data transfer agreement.

26 We gratefully acknowledge all the studies and databases that made GWAS summary

27 data available. Part of data collection and sharing for this project was funded by the

28 Alzheimer’s Disease Neuroimaging initiative (ADNI) (National Institutes of Health Grant

29 U01 AG024904) and DOD ADNI (Department of Defense award number

30 W81XWH-12-2-0012). ADNI is funded by the National Institute on Aging, the National

31 Institute of Biomedical Imaging and Bioengineering and through generous contributions

32 from the following: Alzheimer’s Association; Alzheimer’s Drug Discovery Foundation;

1 Araclon Biotech; BioClinica, Inc.; Biogen Idec Inc.; Bristol-Myers Squibb Company; Eisai
2 Inc.; Elan Pharmaceuticals, Inc.; Eli Lilly and Company; EuroImmune; F. Hoffmann-La
3 Roche Ltd and its affiliated company Genentech, Inc.; Fujirebio; GE Healthcare; IXICO Ltd;
4 Janssen Alzheimer Immunotherapy Research & Development, LLC; Johnson & Johnson
5 Pharmaceutical Research & Development LLC; Medpace, Inc.; Merck & Co., Inc.; Meso
6 Scale Diagnostics, LLC; NeuroRx Research; Neurotrack Technologies; Novartis
7 Pharmaceuticals Corporation; Pfizer Inc.; Piramal Imaging; Servier; Synarc Inc.; and
8 Takeda Pharmaceutical Company. The Canadian Institutes of Health Research is
9 providing funds to support ADNI clinical sites in Canada. Private sector contributions are
10 facilitated by the Foundation for the National Institutes of Health (www.fnih.org). The
11 grantee organization is the Northern California Institute for Research and Education,
12 and the study is coordinated by the Alzheimer's Disease Cooperative Study at the
13 University of California, San Diego. ADNI data are disseminated by the Laboratory for
14 Neuro Imaging at the University of Southern California. Part of the data collection and
15 sharing for this project was funded by the Pediatric Imaging, Neurocognition and
16 Genetics Study (PING) (U.S. National Institutes of Health Grant RC2DA029475). PING is
17 funded by the National Institute on Drug Abuse and the Eunice Kennedy Shriver
18 National Institute of Child Health & Human Development. PING data are disseminated
19 by the PING Coordinating Center at the Center for Human Development, University of
20 California, San Diego. Support for the collection of the PNC datasets was provided by
21 grant RC2MH089983 awarded to Raquel Gur and RC2MH089924 awarded to Hakon
22 Hakonarson. All PNC subjects were recruited through the Center for Applied Genomics
23 at The Children's Hospital in Philadelphia. HCP data were provided by the Human
24 Connectome Project, WU-Minn Consortium (Principal Investigators: David Van Essen
25 and Kamil Ugurbil; 1U54MH091657) funded by the 16 NIH Institutes and Centers that
26 support the NIH Blueprint for Neuroscience Research; and by the McDonnell Center for
27 Systems Neuroscience at Washington University.

28

29 **AUTHOR CONTRIBUTIONS**

30 B.Z., H.Z., and Y.L. designed the study. B.Z. and T.L. performed the experiments and
31 analyzed the data. T.L., J.Z. Y.S., X.W., L.Y., F.Z., and Z.Z. downloaded the datasets,

1 preprocessed MRI and SNP data, and undertook the quantity controls. B.Z., H.Z., and Y.L.
2 wrote the manuscript with feedback from all authors.

3

4 **COMPETETING FINANCIAL INTERESTS**

5 The authors declare no competing financial interests.

6

7 **REFERENCES**

- 8 1. Ritchie SJ, Booth T, Hernández MdCV, Corley J, Maniega SM, Gow AJ, et al. Beyond
9 a bigger brain: Multivariable structural brain imaging and intelligence. *Intelligence*.
10 2015;51:47-56.
- 11 2. Davies G, Marioni RE, Liewald DC, Hill WD, Hagenaars SP, Harris SE, et al.
12 Genome-wide association study of cognitive functions and educational attainment in UK
13 Biobank (N= 112 151). *Molecular psychiatry*. 2016;21(6):758.
- 14 3. van der Meer D, Rokicki J, Kaufmann T, Palomera AC, Moberget T, Alnaes D, et al.
15 Brain scans from 21297 individuals reveal the genetic architecture of hippocampal
16 subfield volumes. *bioRxiv*. 2018:299578.
- 17 4. Caldiroli A, Buoli M, van Haren NE, de Nijs J, Altamura AC, Cahn W. The relationship
18 of IQ and emotional processing with insula volume in schizophrenia. *Schizophrenia*
19 *research*. 2018;202:141-8.
- 20 5. Vreeker A, Abramovic L, Boks MP, Verkooijen S, van Bergen AH, Ophoff RA, et al.
21 The relationship between brain volumes and intelligence in bipolar disorder. *Journal of*
22 *affective disorders*. 2017;223:59-64.
- 23 6. Wigmore EM, Clarke T-K, Howard D, Adams M, Hall L, Zeng Y, et al. Do regional
24 brain volumes and major depressive disorder share genetic architecture? A study of
25 Generation Scotland (n= 19 762), UK Biobank (n= 24 048) and the English Longitudinal
26 Study of Ageing (n= 5766). *Translational psychiatry*. 2017;7(8):e1205.
- 27 7. Elliott LT, Sharp K, Alfaro-Almagro F, Shi S, Miller KL, Douaud G, et al. Genome-wide
28 association studies of brain imaging phenotypes in UK Biobank. *Nature*.
29 2018;562(7726):210.
- 30 8. Hibar DP, Stein JL, Renteria ME, Arias-Vasquez A, Desrivieres S, Jahanshad N, et al.
31 Common genetic variants influence human subcortical brain structures. *Nature*.
32 2015;520(7546):224.

- 1 9. Blokland GA, de Zubicaray GI, McMahon KL, Wright MJ. Genetic and environmental
2 influences on neuroimaging phenotypes: a meta-analytical perspective on twin imaging
3 studies. *Twin Research and Human Genetics*. 2012;15(3):351-71.
- 4 10. Zhao B, Ibrahim JG, Li Y, Li T, Wang Y, Shan Y, et al. Heritability of regional brain
5 volumes in large-scale neuroimaging and genetic studies. *bioRxiv*. 2017:208496.
- 6 11. Boyle EA, Li YI, Pritchard JK. An Expanded View of Complex Traits: From Polygenic
7 to Omnigenic. *Cell*. 2017;169(7):1177-86.
- 8 12. Timpson NJ, Greenwood CM, Soranzo N, Lawson DJ, Richards JB. Genetic
9 architecture: the shape of the genetic contribution to human traits and disease. *Nature*
10 *Reviews Genetics*. 2017.
- 11 13. Zhao B, Zhu H. On genetic correlation estimation with summary statistics from
12 genome-wide association studies. *arXiv*. 2019:arXiv:1903.01301.
- 13 14. Hibar DP, Adams HH, Jahanshad N, Chauhan G, Stein JL, Hofer E, et al. Novel
14 genetic loci associated with hippocampal volume. *Nature communications*.
15 2017;8:13624.
- 16 15. Franke B, Stein JL, Ripke S, Anttila V, Hibar DP, Van Hulzen KJ, et al. Genetic
17 influences on schizophrenia and subcortical brain volumes: large-scale proof of concept.
18 *Nature neuroscience*. 2016;19(3):420-31.
- 19 16. Guadalupe T, Mathias SR, Theo G, Whelan CD, Zwiers MP, Abe Y, et al. Human
20 subcortical brain asymmetries in 15,847 people worldwide reveal effects of age and sex.
21 *Brain imaging and behavior*. 2017;11(5):1497-514.
- 22 17. Ikram MA, Fornage M, Smith AV, Seshadri S, Schmidt R, Debette S, et al. Common
23 variants at 6q22 and 17q21 are associated with intracranial volume. *Nature genetics*.
24 2012;44(5):539.
- 25 18. Bis JC, DeCarli C, Smith AV, Van Der Lijn F, Crivello F, Fornage M, et al. Common
26 variants at 12q14 and 12q24 are associated with hippocampal volume. *Nature genetics*.
27 2012;44(5):545.
- 28 19. Satizabal CL, Adams HH, Hibar DP, White CC, Stein JL, Scholz M, et al. Genetic
29 Architecture of Subcortical Brain Structures in Over 40,000 Individuals Worldwide.
30 *bioRxiv*. 2017:173831.

- 1 20. Davies G, Lam M, Harris SE, Trampush JW, Luciano M, Hill WD, et al. Study of
2 300,486 individuals identifies 148 independent genetic loci influencing general cognitive
3 function. *Nature communications*. 2018;9(1):2098.
- 4 21. Nagel M, Jansen PR, Stringer S, Watanabe K, de Leeuw CA, Bryois J, et al.
5 Meta-analysis of genome-wide association studies for neuroticism in 449,484 individuals
6 identifies novel genetic loci and pathways. *Nature Genetics*. 2018;50(7):920.
- 7 22. Savage JE, Jansen PR, Stringer S, Watanabe K, Bryois J, De Leeuw CA, et al.
8 Genome-wide association meta-analysis in 269,867 individuals identifies new genetic
9 and functional links to intelligence. *Nature genetics*. 2018;50(7):912.
- 10 23. Sudlow C, Gallacher J, Allen N, Beral V, Burton P, Danesh J, et al. UK biobank: an
11 open access resource for identifying the causes of a wide range of complex diseases of
12 middle and old age. *PLoS medicine*. 2015;12(3):e1001779.
- 13 24. Satterthwaite TD, Elliott MA, Ruparel K, Loughhead J, Prabhakaran K, Calkins ME, et
14 al. Neuroimaging of the Philadelphia neurodevelopmental cohort. *Neuroimage*.
15 2014;86:544-53.
- 16 25. Weiner MW, Veitch DP, Aisen PS, Beckett LA, Cairns NJ, Green RC, et al. The
17 Alzheimer's Disease Neuroimaging Initiative: a review of papers published since its
18 inception. *Alzheimer's & Dementia*. 2013;9(5):e111-e94.
- 19 26. Jernigan TL, Brown TT, Hagler DJ, Akshoomoff N, Bartsch H, Newman E, et al. The
20 pediatric imaging, neurocognition, and genetics (PING) data repository. *Neuroimage*.
21 2016;124:1149-54.
- 22 27. Somerville LH, Bookheimer SY, Buckner RL, Burgess GC, Curtiss SW, Dapretto M, et
23 al. The Lifespan Human Connectome Project in Development: A large-scale study of
24 brain connectivity development in 5–21 year olds. *NeuroImage*. 2018;183:456-68.
- 25 28. Avants BB, Tustison NJ, Song G, Cook PA, Klein A, Gee JC. A reproducible evaluation
26 of ANTs similarity metric performance in brain image registration. *Neuroimage*.
27 2011;54(3):2033-44.
- 28 29. Yang J, Zeng J, Goddard ME, Wray NR, Visscher PM. Concepts, estimation and
29 interpretation of SNP-based heritability. *Nature genetics*. 2017;49(9):1304.
- 30 30. de Leeuw CA, Mooij JM, Heskes T, Posthuma D. MAGMA: generalized gene-set
31 analysis of GWAS data. *PLoS computational biology*. 2015;11(4):e1004219.

- 1 31. Watanabe K, Taskesen E, Bochoven A, Posthuma D. Functional mapping and
2 annotation of genetic associations with FUMA. *Nature communications*. 2017;8(1):1826.
- 3 32. Bulik-Sullivan B, Finucane HK, Anttila V, Gusev A, Day FR, Loh P-R, et al. An atlas of
4 genetic correlations across human diseases and traits. *Nature genetics*.
5 2015;47(11):1236.
- 6 33. Buniello A, MacArthur JAL, Cerezo M, Harris LW, Hayhurst J, Malangone C, et al.
7 The NHGRI-EBI GWAS Catalog of published genome-wide association studies, targeted
8 arrays and summary statistics 2019. *Nucleic acids research*. 2018;47(D1):D1005-D12.
- 9 34. Chen C-H, Wang Y, Lo M-T, Schork A, Fan C-C, Holland D, et al. Leveraging genome
10 characteristics to improve gene discovery for putamen subcortical brain structure.
11 *Scientific reports*. 2017;7(1):15736.
- 12 35. Stein JL, Medland SE, Vasquez AA, Hibar DP, Senstad RE, Winkler AM, et al.
13 Identification of common variants associated with human hippocampal and intracranial
14 volumes. *Nature genetics*. 2012;44(5):552.
- 15 36. Furney S, Simmons A, Breen G, Pedroso I, Lunnon K, Proitsi P, et al. Genome-wide
16 association with MRI atrophy measures as a quantitative trait locus for Alzheimer's
17 disease. *Molecular psychiatry*. 2011;16(11):1130.
- 18 37. Baranzini SE, Wang J, Gibson RA, Galwey N, Naegelin Y, Barkhof F, et al.
19 Genome-wide association analysis of susceptibility and clinical phenotype in multiple
20 sclerosis. *Human molecular genetics*. 2008;18(4):767-78.
- 21 38. Fischl B. FreeSurfer. *Neuroimage*. 2012;62(2):774-81.
- 22 39. Hibar DP, Stein JL, Ryles AB, Kohannim O, Jahanshad N, Medland SE, et al.
23 Genome-wide association identifies genetic variants associated with lentiform nucleus
24 volume in N= 1345 young and elderly subjects. *Brain Imaging and Behavior*.
25 2013;7(2):102-15.
- 26 40. Yang J, Lee SH, Goddard ME, Visscher PM. GCTA: a tool for genome-wide complex
27 trait analysis. *The American Journal of Human Genetics*. 2011;88(1):76-82.
- 28 41. Hill W, Marioni R, Maghzian O, Ritchie S, Hagenaars S, McIntosh A, et al. A
29 combined analysis of genetically correlated traits identifies 187 loci and a role for
30 neurogenesis and myelination in intelligence. *Molecular psychiatry*. 2018:1.

- 1 42. Jun G, Ibrahim-Verbaas CA, Vronskaya M, Lambert J-C, Chung J, Naj AC, et al. A
2 novel Alzheimer disease locus located near the gene encoding tau protein. *Molecular*
3 *psychiatry*. 2016;21(1):108.
- 4 43. Luciano M, Hagenaars SP, Davies G, Hill WD, Clarke T-K, Shirali M, et al. Association
5 analysis in over 329,000 individuals identifies 116 independent variants influencing
6 neuroticism. *Nature genetics*. 2018;50(1):6.
- 7 44. Lee JJ, Wedow R, Okbay A, Kong E, Maghzian O, Zacher M, et al. Gene discovery
8 and polygenic prediction from a genome-wide association study of educational
9 attainment in 1.1 million individuals. *Nature genetics*. 2018;50(8):1112.
- 10 45. Edwards TL, Scott WK, Almonte C, Burt A, Powell EH, Beecham GW, et al.
11 Genome-wide association study confirms SNPs in SNCA and the MAPT region as
12 common risk factors for Parkinson disease. *Annals of human genetics*.
13 2010;74(2):97-109.
- 14 46. Turley P, Walters RK, Maghzian O, Okbay A, Lee JJ, Fontana MA, et al. Multi-trait
15 analysis of genome-wide association summary statistics using MTAG. *Nature genetics*.
16 2018:1.
- 17 47. Okbay A, Baselmans BM, De Neve J-E, Turley P, Nivard MG, Fontana MA, et al.
18 Genetic variants associated with subjective well-being, depressive symptoms, and
19 neuroticism identified through genome-wide analyses. *Nature genetics*. 2016;48(6):624.
- 20 48. Pardiñas AF, Holmans P, Pocklington AJ, Escott-Price V, Ripke S, Carrera N, et al.
21 Common schizophrenia alleles are enriched in mutation-intolerant genes and in regions
22 under strong background selection. *Nature genetics*. 2018;50(3):381.
- 23 49. Li Z, Chen J, Yu H, He L, Xu Y, Zhang D, et al. Genome-wide association analysis
24 identifies 30 new susceptibility loci for schizophrenia. *Nature genetics*.
25 2017;49(11):1576.
- 26 50. Marioni RE, Harris SE, Zhang Q, McRae AF, Hagenaars SP, Hill WD, et al. GWAS on
27 family history of Alzheimer's disease. *Translational psychiatry*. 2018;8.
- 28 51. Benjamini Y, Hochberg Y. Controlling the false discovery rate: a practical and
29 powerful approach to multiple testing. *Journal of the royal statistical society Series B*
30 (Methodological). 1995:289-300.

- 1 52. Jansen PR, Watanabe K, Stringer S, Skene N, Bryois J, Hammerschlag AR, et al.
2 Genome-wide Analysis of Insomnia (N= 1,331,010) Identifies Novel Loci and Functional
3 Pathways. *bioRxiv*. 2018:214973.
- 4 53. Skol AD, Scott LJ, Abecasis GR, Boehnke M. Joint analysis is more efficient than
5 replication-based analysis for two-stage genome-wide association studies. *Nature*
6 *genetics*. 2006;38(2):209.
- 7 54. Thompson PM, Stein JL, Medland SE, Hibar DP, Vasquez AA, Renteria ME, et al. The
8 ENIGMA Consortium: large-scale collaborative analyses of neuroimaging and genetic
9 data. *Brain imaging and behavior*. 2014;8(2):153-82.
- 10 55. Consortium IS. Common polygenic variation contributes to risk of schizophrenia
11 and bipolar disorder. *Nature*. 2009;460(7256):748.
- 12 56. Watanabe K, Stringer S, Frei O, Mirkov MU, Polderman TJ, van der Sluis S, et al. A
13 global view of pleiotropy and genetic architecture in complex traits. *bioRxiv*.
14 2018:500090.
- 15 57. Gusev A, Mancuso N, Won H, Kousi M, Finucane HK, Reshef Y, et al.
16 Transcriptome-wide association study of schizophrenia and chromatin activity yields
17 mechanistic disease insights. *Nature genetics*. 2018;50(4):538.
- 18 58. Bycroft C, Freeman C, Petkova D, Band G, Elliott LT, Sharp K, et al. Genome-wide
19 genetic data on ~ 500,000 UK Biobank participants. *BioRxiv*. 2017:166298.
- 20 59. Purcell S, Neale B, Todd-Brown K, Thomas L, Ferreira MA, Bender D, et al. PLINK: a
21 tool set for whole-genome association and population-based linkage analyses. *The*
22 *American Journal of Human Genetics*. 2007;81(3):559-75.
- 23 60. Wang K, Li M, Hakonarson H. ANNOVAR: functional annotation of genetic variants
24 from high-throughput sequencing data. *Nucleic acids research*. 2010;38(16):e164-e.
- 25 61. Consortium G. The Genotype-Tissue Expression (GTEx) pilot analysis: multitissue
26 gene regulation in humans. *Science*. 2015;348(6235):648-60.
- 27 62. Ramasamy A, Trabzuni D, Guelfi S, Varghese V, Smith C, Walker R, et al. Genetic
28 variability in the regulation of gene expression in ten regions of the human brain. *Nature*
29 *neuroscience*. 2014;17(10):1418.
- 30 63. Fromer M, Roussos P, Sieberts SK, Johnson JS, Kavanagh DH, Perumal TM, et al.
31 Gene expression elucidates functional impact of polygenic risk for schizophrenia. *Nature*
32 *neuroscience*. 2016;19(11):1442.

- 1 64. Schmitt AD, Hu M, Jung I, Xu Z, Qiu Y, Tan CL, et al. A compendium of chromatin
2 contact maps reveals spatially active regions in the human genome. Cell reports.
3 2016;17(8):2042-59.
- 4 65. Kundaje A, Meuleman W, Ernst J, Bilenky M, Yen A, Heravi-Moussavi A, et al.
5 Integrative analysis of 111 reference human epigenomes. Nature. 2015;518(7539):317.

6

7

8 **ONLINE METHODS**

9

10 **GWAS participants and phenotypes**

11 We performed GWAS separately on five publicly available datasets: the UK Biobank
12 (UKB) study, the Human Connectome Project (HCP) study, the Pediatric Imaging,
13 Neurocognition, and Genetics (PING) study, the Philadelphia Neurodevelopmental
14 Cohort (PNC) study, and the Alzheimer's Disease Neuroimaging Initiative (ADNI) study.
15 The main GWAS made use of data of 19,629 individuals of British ancestry from the UKB
16 study, and the other four GWAS were performed on individuals of European ancestry,
17 see **Supplementary Table 24** for a summary of sample size of each GWAS.

18

19 The raw MRI, covariates and SNP data were downloaded from each data resource. We
20 processed the MRI data locally using consistent procedures via advanced normalization
21 tools (ANTs) to generate ROI volume phenotypes for each dataset. The processing steps
22 were detailed in Zhao, Ibrahim (10) and we removed three ROIs (X5th ventricle and
23 left/right lesion) with missing rates > 99%. For each phenotype and continuous covariate
24 variable, we further removed values greater than five times the median absolute
25 deviation from the median value. All individuals were aged between 3 and 92 years.
26 More information about study cohorts can be found in **Supplementary Table 25** and
27 **Supplementary Note**.

28

29 **Heritability estimation and Genome-wide association analysis**

30 We estimated the proportion of variation explained by all autosomal SNPs in UKB with
31 using univariate GCTA-GREML analysis (40). The adjusted covariates included age (at
32 imaging), age-squared, gender, age-gender interaction, age-squared-gender interaction,

1 TBV (for ROIs other than TBV itself), as well as the top 40 genetic principle components
2 (PCs) provided by UKB ((58), Data-Field 22009). We performed GWAS for each ROI
3 volume with PLINK (59). The same set of covariates as in GCTA-GREML analysis were
4 adjusted. GWAS were also separately performed on PING, PNC, ADNI, and HCP data. In
5 these four datasets, we adjusted for age, age-squared, gender, age-gender interaction,
6 age-squared-gender interaction, TBV (for ROIs other than TBV itself), and top ten
7 genetic PCs estimated from the SNP data. We also adjusted for the Alzheimer's disease
8 status in ADNI GWAS.

9

10 **Genomic risk loci characterization and comparison with previous findings**

11 Genomic risk loci were defined using FUMA (31) online platform (version: 1.3.4). We
12 input the UKB GWAS summary statistics obtained from PLINK (59). FUMA first identified
13 independent significant SNPs, which were defined as SNPs with a p-value smaller than
14 the predefined threshold and independent of other significant SNPs at R-squared < 0.6.
15 Using these independent significant SNPs, FUMA then constructed LD block for
16 independent significant SNPs by tagged all SNPs that had a MAF ≥ 0.0005 and were in
17 LD (R-squared ≥ 0.6) with at least one of the independent significant SNPs. These SNPs
18 included those from the 1000 Genomes reference panel and may not have been
19 included in the present study. Based on these independent significant SNPs,
20 (independent) lead SNPs were also identified as those that were independent from each
21 other (R-squared < 0.1). If LD blocks of independent significant SNPs were closed (<250
22 kb based on the closest boundary SNPs of LD blocks), they were merged to a single
23 genomic locus. Thus, each genomic locus could contain more than one independent
24 significant SNPs and lead SNPs. More details can be found in Watanabe, Taskesen (31).
25 Independent significant SNPs and all the tagged SNPs were subsequently searched by
26 FUMA on NHGRI-EBI GWAS catalog ((33), version: 2019-01-31) to look for their reported
27 SNP associations (p-value < 9×10^{-6}) with any traits.

28

29 **Gene-based association analysis, functional annotation and gene-property analysis**

30 Gene-based association analysis was carried out for 18,796 protein-coding genes using
31 MAGMA (30), which was also implemented in FUMA (31). SNPs were mapped according

1 to their psychical positions, then the gene-based p-values were calculated by the GWAS
2 summary statistics of mapped SNPs.

3

4 In functional annotation and mapping analysis, SNPs signals were annotated with their
5 biological functionality and then were linked to genes by a combination of positional,
6 eQTL, and 3D chromatin interaction mappings (31). Specifically, independent significant
7 SNPs and all the tagged SNPs were first annotated for functional consequences on gene
8 functions (e.g., intergenic, intronic, exonic) using ANNOVAR (60). Functionally-annotated
9 SNPs were then mapped to 35,808 candidate genes based on physical position on the
10 genome (tissue/cell types for 15-core chromatin state: brain), eQTL associations (tissue
11 types: GTEx v7 brain (61), BRAINEAC (62), and CommonMind Consortium (63)) and
12 chromatin interaction mapping (built-in chromatin interaction data: dorsolateral
13 prefrontal cortex, hippocampus (64); annotate enhancer/promoter regions: E053-E082
14 brain (65)). We used default values for all other parameters.

15

16 For the detected genes, we performed lookups on NHGRI-EBI GWAS catalog ((33),
17 version: 2019-01-31) again to explore the previously reported associations with the
18 same or other traits. We focused on traits including cognitive functions (such as general
19 cognitive ability, cognitive performance, and empathy quotient), intelligence,
20 educational attainment, math ability (such as highest math class taken and self-reported
21 math ability), reaction time, neuroticism, neurodegenerative diseases (such as
22 Alzheimer's disease and Parkinson's disease), and neuropsychiatric disorders (such as
23 major depressive disorder, Schizophrenia, and bipolar disorder). For the 14 brain tissues
24 (GTEx v7, (61)), we also performed gene-priority analysis via MAGMA (30). That is, for
25 each candidate gene, whether its tissue-specific expression levels can be linked to the
26 strength of its association with ROI volumes.

27

28 **Meta-analysis of GWAS results**

29 We meta-analyzed the UKB, PING, PNC, ADNI, and HCP GWAS summary results by
30 METAL (<https://genome.sph.umich.edu/wiki/METAL>) with the sample-size weighted
31 approach. Since the sample sizes of other four datasets were small, we removed the
32 SNPs that were not presented in the UKB data.

1

2 **Genetic correlation estimation with LDSC**

3 The LD Hub (v1.9.1, <http://ldsc.broadinstitute.org/ldhub/>) was used to estimate the
4 genetic correlation between several UKB ROIs volumes and their corresponding traits
5 studied in the ENIGMA consortium (54). Then the LDSC software (v1.0.0,
6 <https://github.com/bulik/ldsc>) was used to estimate the pairwise genetic correlation
7 with 50 sets of collected GWAS summary statistics. We used the pre-calculated LD
8 scores provided by LDSC (<https://data.broadinstitute.org/alkesgroup/LDSCORE/>), which
9 were computed using 1000 Genomes European data. We used HapMap3 SNPs and
10 removed all SNPs on chromosome 6 in the MHC region.

11

12 **Polygenic scoring**

13 Polygenic profiles were created to examine the out-of-sample prediction power of the
14 GWAS results. Specifically, we used PLINK (59) to generate risk scores in testing data by
15 summarizing across pruned (window size 50, step 5, R-squared = 0.2) SNP alleles,
16 weighed by their effect sizes estimated from training data. We randomly divided the
17 19,629 UKB individuals into ten folds, then used nine of these folds as training data to
18 rerun GWAS, and created polygenic profiles on the individuals in the remaining fold,
19 which served as testing data. We repeated this procedure ten times such that each fold
20 alternated to serve as the testing data for exactly one time. Then we used the UKB
21 GWAS results to perform prediction on ADNI, PING, PNC and HCP data. The prediction
22 accuracy was evaluated on all samples in the four testing sets (with phenotype and SNP
23 data available), not limited to individuals of European ancestry used in GWAS. We tried
24 five p-value thresholds for SNP predictor selection: 1, 0.5, 0.05, 5×10^{-4} and 5×10^{-8} . The
25 association between polygenic profile and brain volume was estimated and tested in
26 linear regression model, adjusting for the effects of age and gender. The additional
27 variance of brain volume that can be explained by polygenic profile was used to
28 measure the prediction power.

29

30 **Data availability**

31 All UKB and meta-analysis GWAS summary statistics of 101 ROI volumes can be found at:
32 <https://med.sites.unc.edu/big2/data/gwas-summary-statistics/>.

1

2 **Figure and Table Legends**

3

4 Figure 1. Number of independent significant SNP associations discovered in UKB GWAS
5 at different significance levels. Outer layer: p-value $<5*10^{-8}$; middle layer: p-value
6 $<5*10^{-9}$; and inner layer: p-value $<4.9*10^{-10}$.

7

8 Figure 2. Genes identified in gene-based association analysis of ROI volumes that have
9 been linked to cognitive traits and mental health disease/disorders in previous GWAS.

10

11 Figure 3. Selected pairwise genetic correlations between ROI volumes and other traits

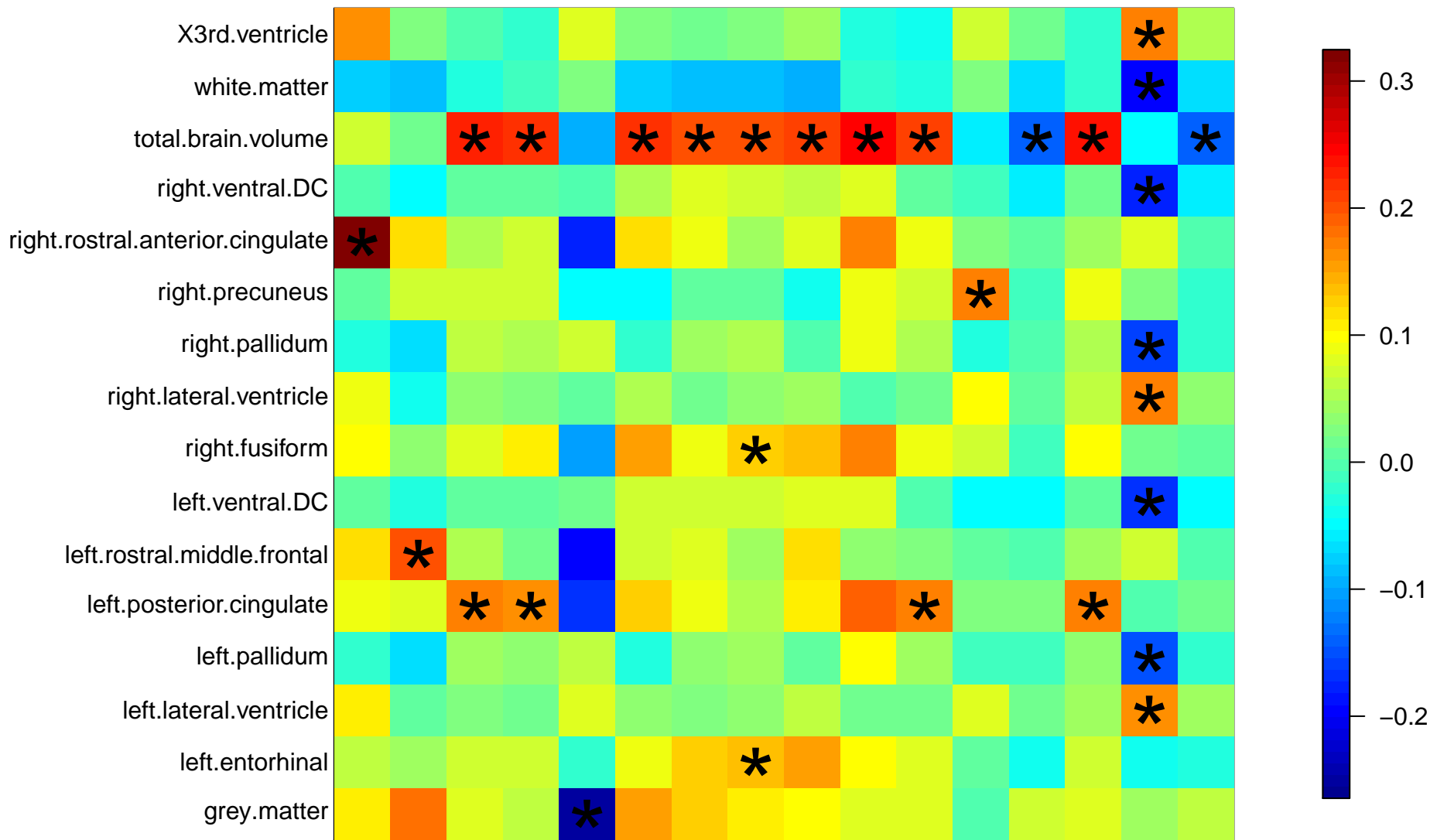
12

13 Table 1. List of significant genetic risk loci identified by UKB GWAS at $4.9*10^{-10}$
14 significant level. RSID: rsID of the top lead SNP; Position: position of top lead SNP.

15

16 Table 2. List of significant genes identified by gene-based association analysis in UKB
17 data at $2*10^{-8}$ significant level.

*Significant after adjusting for multiple testing (n.test=4900) at 0.05 level



Autism spectrum disorder (PGC, n=46,351)
 Bipolar disorder (PGC, n=41,653)
 Cognitive cognitive function (CCACE, n=282,014)
 Depressive performance (SSGAC, n=257,828)
 College completion (SSGAC, n=161,460)
 Educational attainment (SSGAC, n=126,559)
 Educational attainment (SSGAC, n=293,723)
 Education years (SSGAC, n=766,345)
 Intelligence (CTG, n=126,559)
 Intelligence (CTG, n=78,308)
 Neuroticism-(irritable) (CTG, n=269,867)
 Neuroticism-(worry) (CTG, n=366,726)
 Numerical reasoning (CCACE, n=372,869)
 Reaction time (CCACE, n=168,033)
 Worry (CTG, n=330,069)
 Worry (CTG, n=348,219)

RSID	ROI	CHR	Position	p-value	p-value (second ROI, if any)	p-value (third ROI, if any)	Start position of the locus	End position of the locus
rs2817145	left.caudate	1	3133422	9.29E-16			3118674	3149789
rs2817145	right.caudate	1	3133422	7.69E-13			3121877	3149789
rs3120124	left.pallidum	1	43764165	7.95E-11			43760070	43949718
rs6658111	X4th.ventricle	1	47980916	2.60E-18			47712057	47980916
rs6658111	left.parahippocampal	1	47980916	2.62E-16			47915175	47993332
rs6658111	CSF	1	47980916	3.58E-10			47974123	47980916
rs3176459	left.amygdala	1	51437247	1.48E-10			50828316	51526458
rs12072311	left.cerebellum.exterior	1	51572465	1.51E-12			50882506	52215089
rs12072311	right.cerebellum.exterior	1	51572465	5.49E-14			50882506	52368501
rs74091739	cerebellar.vermal.lobules.VIII.X	1	76028726	3.21E-45			75818830	76095959
rs2748444	cerebellar.vermal.lobules.I.V	1	76010959	1.23E-19			75946751	76091842
rs76934732	cerebellar.vermal.lobules.VI.VII	1	76013268	2.72E-11			75946751	76073887
rs11392431, rs2991716	right.inferior.parietal, left.inferior.parietal	1	88423056, 88423966	3.10E-10	3.22E-10		88196463	88435308
rs1044595	white.matter	1	180943529	4.64E-13			180940588	181017348
rs1452628	grey.matter	1	215139887	7.34E-12			215134041	215327772
rs1030088	left.inferior.temporal	2	65937745	4.22E-10			65937041	65999623
rs34111434	right.transverse.temporal	2	150048607	3.60E-10			149945701	150084200
rs5835889	right.hippocampus	2	162845572	3.78E-10			162314229	162891848
rs5835889	left.hippocampus	2	162845572	9.80E-12			162796517	162891848
rs759663	cerebellar.vermal.lobules.VIII.X	2	208080975	2.76E-12			208017033	208102505
rs2234675	left.cerebellum.exterior	2	223085955	1.19E-10			223046616	223085955
rs12636275	right.inferior.temporal	3	89523038	9.00E-11			89451721	89751353
rs12633109	right.vessel	3	146392141	2.89E-11			146337667	146396844
rs2279829	right.pars.triangularis	3	147106319	4.52E-14			147090583	147224629
rs2279829	left.pars.triangularis	3	147106319	3.56E-10			147095294	147224629
rs2279829	left.postcentral	3	147106319	1.87E-10			147095294	147140680
rs2279829	right.postcentral	3	147106319	7.02E-12			147095294	147268599
rs34859790, rs61500084, rs61500084	left.inferior.lateral.ventricle, left.lateral.ventricle, right.lateral.ventricle	3	190652830, 190636749,19063 6749	4.39E-11	2.80E-13	2.59E-17	190591418	190678743
rs10706986	left.accumbens.area, right.accumbens.area	3	190646282	2.04E-10	1.40E-13		190592836	190678743
rs13073466	cerebellar.vermal.lobules.VIII.X	3	192617930	1.38E-10			192613518	192716379
rs10034561	cerebellar.vermal.lobules.VIII.X	4	66701964	2.28E-16			66629087	66966038
rs17755998	cerebellar.vermal.lobules.VI.VII	4	66714289	1.08E-21			66653473	67034895
rs13107325	left.accumbens.area	4	103188709	5.05E-19			102702364	103387161
rs13107325	right.accumbens.area	4	103188709	9.64E-16			102702364	103388441
rs13107325	white.matter	4	103188709	2.52E-13			103001649	103387161
rs10478102	cerebellar.vermal.lobules.VIII.X	5	112398770	4.99E-15			112379434	112442272
rs152234	white.matter	5	179335060	2.73E-12			179287576	179370127
rs2819861	left.putamen	6	45424940	8.20E-12			45407654	45510107
rs35405209	right.pallidum	6	45428508	2.42E-10			45407654	45461253
rs12215796	Brain.stem	6	55715715	4.20E-10			55679959	55717728
rs9296804	left.cerebellum.white.matter	6	55717728	4.14E-10			55712608	55717728
rs9345125	right.precentral	6	92002653	1.14E-10			92002569	92010010
rs2153960	Brain.stem, left.ventral.DC, right.ventral.DC	6	108988184	7.69E-12	1.05E-11	6.32E-12	108861264	109020032
rs2764264	total.brain.volume	6	108934461	5.16E-13			108861264	109019323
rs11759026	total.brain.volume	6	126792095	1.25E-16			126659043	127167072
rs62435771	CSF	6	169470668	3.26E-10			169469707	169555989
rs368699386	left.lateral.ventricle	7	2803883	1.09E-14			2745766	2912928
rs368699386, rs529794364	X3rd.ventricle, right.lateral.ventricle	7	2803883, 2791033	3.28E-12	3.17E-12		2752152	2912928
rs151057105	left.ventral.DC, right.ventral.DC	7	54944920	7.38E-14	5.51E-14		54909928	55015505
rs4006770	cerebellar.vermal.lobules.VIII.X	7	103361695	8.81E-26			103200019	103396186
rs12705150	cerebellar.vermal.lobules.VI.VII	7	103356275	2.53E-11			103356062	103373126
rs142005327	white.matter	7	120969969	2.21E-11			120954908	121040782
rs7778054	cerebellar.vermal.lobules.I.V	7	156095814	1.40E-11			156066471	156170722
rs196814	left.pallidum	8	24716594	2.18E-10			24679371	24764896
rs13268108	right.cerebellum.exterior	8	142039586	1.30E-10			142033034	142042870
rs11789773	right.postcentral	9	76157130	1.10E-10			75849823	76193770
rs12344396	left.cerebellum.white.matter	9	118921327	3.75E-16			118917007	119098518
rs1405	Brain.stem	9	118954624	7.48E-16			118917007	119002278
rs72754248	left.cerebellum.exterior, right.cerebellum.exterior	9	119061396	7.72E-39	1.25E-37		118917007	119134875
rs72754266	right.cerebellum.white.matter	9	119093757	2.51E-15			118917007	119098518
rs147269950	X4th.ventricle	9	119098518	1.00E-14			119061396	119098518
rs7030607	left.hippocampus, right.hippocampus	9	119245183	6.81E-19	1.37E-14		119241165	119479868
rs77641763	cerebellar.vermal.lobules.VIII.X	9	140265782	1.20E-10			140241209	140278206
rs4748994	left.caudate	10	25300609	3.10E-11			25233290	25377328
rs6584542	total.brain.volume	10	104995495	3.69E-14			104965551	105176914
rs4752582	left.cerebellum.exterior	10	123443605	1.82E-10			123443605	123443605
rs4046908	white.matter	11	1483117	7.69E-11			1472475	1632590
rs10770131	left.lateral.ventricle, right.lateral.ventricle	11	10682248	5.99E-12	1.89E-11		10655021	10699750
rs1187162	left.caudate	11	92011126	4.02E-11			92001738	92036512
rs1187162	right.caudate	11	92011126	1.38E-10			92001738	92315907
rs688968	left.putamen, right.putamen	11	117406739	7.36E-13	5.10E-11		117383215	117429845

rs7936928	CSF	11	130279168	1.28E-16		130260673	130297957
rs11062908	left.amygdala, right.amygdala	12	4005222	1.42E-16	1.34E-16	4004752	4013260
rs17178006	right.hippocampus	12	65718299	2.84E-32		65386792	66065136
rs17178006	left.hippocampus	12	65718299	9.50E-33		65400292	66065136
rs17178006	right.amygdala	12	65718299	3.93E-10		65718299	65874956
rs8756	total.brain.volume	12	66359752	4.42E-14		66326943	66389968
rs11111094	left.cerebellum.white.matter, right.cerebellum.white.matter	12	102328806	3.03E-31	9.74E-28	102096012	102946220
rs11111094	Brain.stem	12	102328806	3.54E-22		102319002	102866662
rs35872193	right.cerebellum.exterior	12	102442428	9.61E-12		102394872	102962583
rs12146713	left.lateral.ventricle, right.lateral.ventricle	12	106476805	1.86E-11	1.88E-13	106476805	106510413
rs10778498	Brain.stem	12	107063340	5.77E-14		106960182	107522203
rs146607495	left.hippocampus	12	117319202	1.24E-23		117229539	117506632
rs146607495	right.hippocampus	12	117319202	5.04E-25		117234676	117528064
rs17126556	CSF	14	53942788	6.98E-12		53917808	53996110
rs8014725	right.putamen	14	56186953	2.81E-32		55921561	56206214
rs8017172	left.putamen	14	56199048	2.57E-28		55998163	56206214
rs8014725	left.pallidum	14	56186953	7.17E-11		56177508	56201197
rs76341705	left.pericalcarine	14	59628679	9.97E-21		59449138	59916960
rs76341705	left.cuneus	14	59628679	2.90E-12		59585670	59669948
rs147148763, rs5809016	left.precuneus, right.precuneus	14	59631075, 59627434	2.87E-10	4.22E-12	59588323	59860859
rs5809016, rs73313052	left.inferior.parietal, right.pericalcarine	14	59627434, 59625997	5.71E-11	2.56E-10	59588323	59669948
rs2033939	right.precentral	15	39633904	4.46E-63		39355860	39670175
rs2033939	left.precentral	15	39633904	5.11E-73		39534404	39670175
rs28520337, rs4924345	left.supramarginal, right.supramarginal	15	39647894, 39639898	1.86E-10	2.18E-12	39617295	39664000
rs34680120	left.superior.parietal	15	39664000	5.81E-11		39631771	39664000
rs4775006	X4th.ventricle	15	58215727	1.01E-20		58188859	58385264
rs12921170	right.lateral.ventricle	16	87227397	4.01E-24		87211783	87357985
rs4843552	left.lateral.ventricle	16	87233516	2.93E-22		87211963	87266245
rs4843550, rs4843560	X3rd.ventricle, X4th.ventricle	16	87236383, 87225143	1.86E-14	4.78E-17	87220694	87265438
rs3833159	right.precuneus	17	27953390	3.89E-11		27925812	28553639
rs3110494	left.insula	17	27976597	1.01E-13		27935546	28553639
rs3110494	right.insula	17	27976597	5.44E-13		27935546	28538715
rs78777685	cerebellar.vermal.lobules.I.V	17	35257232	5.46E-23		35215422	35266724
rs118087478	total.brain.volume	17	44051589	1.03E-13		43463493	44865603
rs11665242, rs6508230	left.putamen, right.putamen	18	50907127, 50884924	2.25E-15	2.52E-15	50555225	51061399
rs60575064	X3rd.ventricle	19	33565344	9.33E-12		33525467	33631912
rs35255138	cerebellar.vermal.lobules.I.V	19	41197268	3.51E-11		41148797	41197268
rs6121038	right.pallidum	20	30254773	2.20E-12		29420066	30437522
rs6121038	left.pallidum	20	30254773	1.17E-12		29509439	30439298
rs6121038	right.putamen	20	30254773	3.01E-10		30235302	30434084
rs6062237, rs6062264	right.ventral.DC, left.ventral.DC	20	61154437, 61154871	2.55E-12	2.16E-14	61141981	61158050
rs34134374	left.lateral.ventricle	22	38138284	4.52E-10		38102776	38304858

LRR37A2	ENSG00000238083	total.brain.volume	17	44588877	44633016	4.91E-11					
LRR49	ENSG00000137821	white.matter	15	71145578	71342414	4.07E-09					
LYPD6B	ENSG00000150556	right.transverse.temporal	2	149894621	150071776	4.08E-11					
MAPT	ENSG00000186868	total.brain.volume	17	43971748	44105700	1.59E-10					
MCC	ENSG0000011444	cerebellar.vermal.lobules.VIII.X	5	112357796	112824527	2.90E-12					
METTL10	ENSG00000203791	left.isthmus.cingulate, left.hippocampus, right.hippocampus	10	126436718	126480439	4.21E-09	1.16E-08	9.88E-09			
MITF	ENSG00000187098	white.matter	3	69788586	70017488	1.74E-08					
MPL	ENSG00000117400	left.pallidum	1	43803478	43818443	3.95E-09					
MR1	ENSG00000153029	white.matter	1	181003067	181031074	7.37E-10					
MSRB3	ENSG00000174099	right.inferior.parietal, left.hippocampus, right.hippocampus	12	65672423	65882024	4.77E-11	7.67E-23	3.34E-24			
MTX1	ENSG00000173171	white.matter	1	155178490	155183615	9.35E-10					
MYLK2	ENSG00000101306	left.pallidum, right.pallidum, right.pallidum	20	30407111	30422492	2.42E-10	4.10E-09	3.93E-10			
NADK	ENSG00000008130	right.ventral.DC	1	1682671	1711896	4.84E-09					
NINL	ENSG00000101004	left.pallidum	20	25433341	25566153	2.76E-10					
NOL12	ENSG00000100101	X3rd.ventricle, left.lateral.ventricle	22	38077680	38170137	9.00E-09	1.04E-08				
NSF	ENSG00000073969	total.brain.volume	17	44668035	44834830	4.76E-11					
NSRP1	ENSG00000126653	left.insula, right.precuneus, right.insula	17	28442539	28513493	5.76E-11	6.51E-10	1.66E-10			
NUMBL	ENSG00000105245	cerebellar.vermal.lobules.I.V	19	41172596	41196877	5.12E-09					
NUP160	ENSG00000030066	left.pallidum, right.pallidum	11	47799639	47870107	2.98E-10	1.55E-10				
NUP210L	ENSG00000143552	left.inferior.lateral.ventricle	1	153965161	154127592	7.17E-10					
NUP37	ENSG00000075188	left.cerebellum.white.matter, right.cerebellum.exterior, right.cerebellum.white.matter	12	102467967	102513902	5.19E-13	1.42E-10	3.01E-13			
NUP43	ENSG00000120253	left.hippocampus, right.hippocampus	6	150045451	150078081	9.04E-09	6.67E-09				
ORC5	ENSG00000164815	left.entorhinal	7	103766788	103848495	9.01E-10					
PH42	ENSG00000072682	CSF	5	131527531	131631008	5.35E-09					
PANX2	ENSG00000073150	left.fusiform	22	50609160	50618723	5.30E-10					
PAPPA	ENSG00000182752	cerebellar.vermal.lobules.I.V, Brain.stem, left.cerebellum.exterior, left.cerebellum.white.matter, right.cerebellum.exterior, right.cerebellum.white.matter	9	118916083	119164601	1.53E-09	2.88E-13	7.38E-22	1.15E-18	1.54E-20	6.52E-18
PARPBP	ENSG00000185480	left.cerebellum.white.matter, right.cerebellum.exterior, right.cerebellum.white.matter	12	102513956	102591298	2.19E-10	1.34E-09	3.42E-11			
PCGF6	ENSG00000156374	total.brain.volume	10	105062553	105110891	1.79E-11					
PDCD11	ENSG00000148843	total.brain.volume	10	105156405	105206049	5.17E-10					
PIGF	ENSG00000151665	cerebellar.vermal.lobules.I.V	2	46808076	46844258	1.25E-08					
PITPNM2	ENSG00000090975	cerebellar.vermal.lobules.I.V	12	123468027	123634562	8.88E-09					
PLK1H1	ENSG00000225190	total.brain.volume	17	43513266	43568115	1.58E-09					
PRDM16	ENSG00000142611	left.caudate	1	2985732	3355185	3.58E-09					
PRDM5	ENSG00000138738	grey.matter	4	121606074	121844025	1.44E-10					
PYGB	ENSG00000100994	left.pallidum	20	25228705	25278650	3.47E-10					
RAPGEF2	ENSG00000109756	left.caudate	4	160025330	160281321	1.46E-09					
RELN	ENSG00000189056	cerebellar.vermal.lobules.VIII.X	7	103112231	103629963	2.08E-28					
RFX4	ENSG00000111783	Brain.stem, left.ventral.DC, right.ventral.DC	12	106976685	107156581	1.88E-16	1.19E-09	6.91E-10			
RHPN2	ENSG00000131941	X3rd.ventricle	19	33469499	33555794	2.23E-11					
RIC8B	ENSG00000111785	Brain.stem	12	107168373	107283090	1.43E-10					
RNF11	ENSG00000123091	left.cerebellum.exterior, right.cerebellum.exterior	1	51701943	51739127	2.78E-12	2.14E-12				
RP11-12J10.3	ENSG00000258539	left.isthmus.cingulate	10	126305649	126480296	2.82E-09					
RP11-144F15.1	ENSG00000257545	Brain.stem, left.ventral.DC, right.ventral.DC	12	106889736	107168696	7.66E-19	1.26E-10	4.00E-11			
RP11-20IK10.3	ENSG00000273088	white.matter	1	155141885	155159748	6.36E-09					
SELO	ENSG00000073169	right.ventral.DC	22	50639408	50656045	1.58E-08					
SLC39A1	ENSG00000143570	left.inferior.lateral.ventricle	1	153931575	153940188	1.26E-08					
SLC44A5	ENSG00000137968	cerebellar.vermal.lobules.I.V, cerebellar.vermal.lobules.VIII.X	1	75667816	76076801	1.06E-09	3.13E-23				
SLC6A4	ENSG00000108576	left.insula, right.precuneus, right.insula	17	28521337	28563020	2.87E-10	4.16E-09	6.26E-10			
SPPL2C	ENSG00000185294	total.brain.volume	17	43922256	43924438	5.68E-11					
SOSTM1	ENSG00000161011	white.matter	5	179233388	179265078	1.91E-08					
SSH2	ENSG00000141298	left.insula, right.precuneus, right.insula	17	27952956	28257294	2.68E-12	1.06E-09	5.60E-12			
STH	ENSG00000256762	total.brain.volume	17	44076616	44077060	1.78E-12					
STK17A	ENSG00000164543	cerebellar.vermal.lobules.I.V	7	43622357	43666385	8.06E-09					
STX6	ENSG00000135823	right.pallidum, white.matter	1	180941861	180992047	1.94E-09	5.24E-13				
SZT2	ENSG00000198198	left.pallidum	1	43855553	43918321	6.89E-10					
TAF5	ENSG00000148835	total.brain.volume	10	105127724	105148822	9.27E-11					
TBC1D9B	ENSG00000197226	white.matter	5	179289066	179334859	2.65E-10					
THBS3	ENSG00000169231	grey.matter, white.matter	1	155165379	155178842	5.84E-09	1.22E-09				
THNSL1	ENSG00000185875	left.caudate	10	25305587	25315593	1.09E-08					
TIE1	ENSG00000060656	left.pallidum	1	43766664	43788779	1.57E-09					
TPX2	ENSG00000088325	left.putamen, left.pallidum, right.putamen, right.pallidum	20	30327074	30389608	6.30E-09	1.24E-11	9.84E-10	2.04E-11		
TRIOBP	ENSG00000100106	X3rd.ventricle, left.lateral.ventricle	22	38093011	38172563	6.01E-09	5.39E-09				
TTC39A	ENSG00000085831	left.cerebellum.exterior, right.cerebellum.exterior	1	51752930	51810788	2.82E-12	7.64E-13				
USMG5	ENSG00000173915	total.brain.volume	10	105148798	105156223	5.48E-10					
VCAN	ENSG00000038427	white.matter	5	82767284	82878122	9.12E-11					
WIF1	ENSG00000156076	left.hippocampus, right.hippocampus	12	65444406	65515346	8.26E-15	5.59E-16				
WNT3	ENSG00000108379	total.brain.volume	17	44839872	44910520	6.82E-11					
ZIC1	ENSG00000152977	left.pars.triangularis, right.pars.triangularis, right.postcentral	3	147111209	147228080	3.42E-09	5.55E-12	7.78E-09			
ZIC4	ENSG00000174963	left.pars.triangularis, left.postcentral, right.pars.triangularis, right.postcentral	3	147103833	147124647	1.55E-09	1.89E-08	2.26E-12	4.98E-09		
ZNF474	ENSG00000164185	left.vessel	5	121465208	121515312	5.17E-09					